Results of the Implementation of Model Predictive Control in a Large Administrative Building for Energy Efficiency and Comfort Optimization

Svenne FREUND[1*], Gerhard SCHMITZ[1], Arne SPEERFORCK[1]

[1] Hamburg University of Technology, Institute of Engineering Thermodynamics, Hamburg, Germany
Phone: +4940 42878-2596, E-mail: svenne.freund@tuhh.de

* Corresponding Author

ABSTRACT

This paper presents the results from a practical implementation of a Model Predictive Control (MPC) strategy in a large administrative building, aiming to optimize both thermal comfort and energy efficiency of the building. The core of this control strategy consists of zones models that describe the thermal and dynamic behavior of individual reference zones within the building. A hybrid gray-box modeling approach is used, combining a simplified physics-based model structure with a parameter identification using data collected from the building operation. The MPC controller was implemented in multiple sections of the building during a six-month period, controlling the supply temperature and pumps of heating circuits for thermally activated building systems (TABS). Compared to the default conventional control strategy, a monthly average saving in heating energy in the range of 5 % to 42 % can be measured during the test periods. Furthermore, an improvement in thermal comfort compared to the previous operational years can also be demonstrated. In the reference zones, a significantly higher proportion of indoor air conditions within the highest comfort category according to DIN EN 16798 is achieved.

1. INTRODUCTION

Worldwide, the operation of buildings accounts for 30 % of final energy consumption and 26 % of global energy-related greenhouse gas (GHG) emissions (IEA, 2023). The transformation towards environmentally friendly and energy-efficient buildings is therefore crucial for global climate protection. Besides decarbonizing the heating and electricity sector, avoiding GHG emissions by reducing the energy requirements of buildings is an effective climate protection measure. In addition to energy-efficient refurbishment measures, hardware or software-based measures on the control and regulation systems of building automation systems represent an effective approach for reducing the energy requirement of buildings (Gyalistras et al., 2010). Especially in modern, large, and often highly-insulated buildings, which are designed and constructed with high standards for energy efficiency and comfort, the influence of the control strategy on the overall energy-efficiency is often underestimated. In most of these buildings, simple, rule-based control (RBC) strategies are implemented that are not or insufficiently adjusted to the underlying system and therefore do not exploit the full potential (Treado & Chen, 2013).

Model Predictive Control (MPC) is an advanced control strategy that has been increasingly investigated in recent years for the energy-efficient and intelligent control of buildings and has been identified as a promising approach (Sofos et al., 2020). MPC has been shown to be capable of improving the thermal comfort of building occupants, while simultaneously reducing the energy demand of buildings in a range of 15 % to 50 % (Serale et al., 2018). A reason for the effectiveness of MPC is the consideration of building dynamics via one or more dynamic building models that can describe the thermal behavior of the building accurately, as well as the integration of predictions of external and internal disturbances (Drgoňa et al., 2020). However, the implementation of MPC is in practice still far from trivial and still requires considerable effort. Many studies have analyzed the potential of MPC based on simulations, but the number of "real-world" implementations is still limited, especially for occupied and fully operated large-sized buildings (Thieblemont et al., 2017).

This paper presents a field test demonstration of MPC over a period of six months in a modern large-sized, energy-efficient office building in Northern Germany. In a distinctive experimental configuration, a detailed comparison between building sections controlled by MPC and RBC is conducted. This comparison takes places under identical

environmental and operational conditions, focusing on aspects such as heating energy demand and thermal comfort. In contrast to (Freund & Schmitz, 2021), this paper considers an entire heating period of six months and presents a comprehensive comparison with the previous six years of building operation.

2. BUILDING DESCRIPTION

The demonstration building is a large, energy-efficient administrative building located in Northern Germany with a net floor area of 46 500 m^2 and approximately 1,500 workplaces. It was completed in 2013 as part of the International Building Exhibition. The building has been subject to intensive monitoring as part of the Energy-Optimized Building (EnOB) research initiative since the beginning of its operational phase.

Figure 1 shows an exterior view of the building and a schematic of the building concept. The building consists of two 5-storey side wings and a central 13-storey tower. The north wing is divided into three sections, while the west wing is divided into four sections. These sections are referred to as "Building A" to "Building H" with "Building E" as the high-rise.

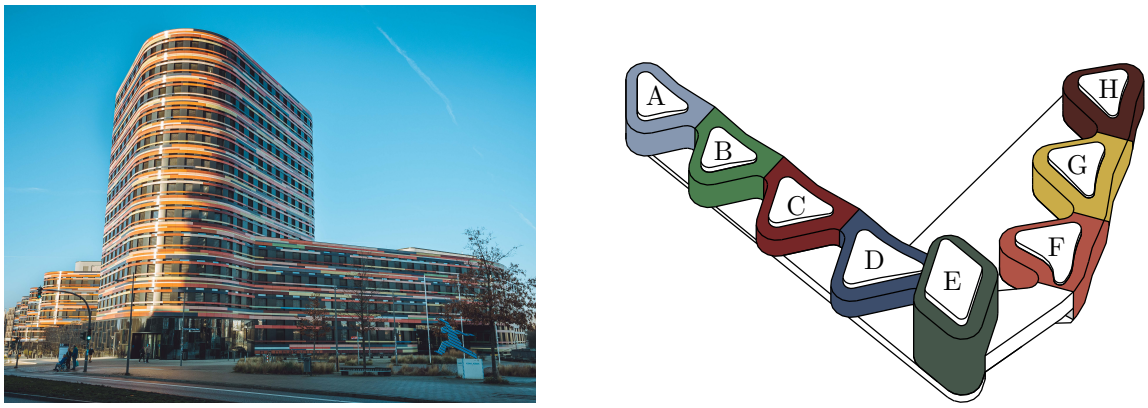

(a) Exterior view. **(b)** Schematic illustration.

Figure 1: Exterior view of the office building (a) and schematic illustration (b) with named building sections.

The building was designed and constructed with high standards for primary and heating energy consumption as well as user comfort. The energy performance targets were set with a maximum annual primary energy demand of 70 kWh/(m^2a) and a maximum annual heating energy demand of 15 kWh/(m^2a).

2.1 Heating system

The building's heating system in mainly based on shallow geothermal energy through the thermal activation of the building's foundation piles, coupled with two electric ground-source heat pumps. The two heat pumps, with a thermal nominal capacity of 232 kW each, serve for the base load supply. A district heating integration with a thermal nominal capacity of 750 kW is utilized for peak load coverage and domestic hot water supply.

The building is primarily heated via thermoactive ceilings (TAC), implemented as the thermal activation of the concrete core of the floor slabs with maximum supply temperature of 32 °C (see Figure 2a). Some offices are also equipped with underfloor heating. For controlled mechanical ventilation, the offices are supplied with tempered supply air in heating mode.

In summer mode, the building is passively cooled by thermoactive ceilings supplied with chilled water, ranging from 18 °C to 20 °C. The mechanical ventilation is replaced by natural ventilation through windows or night ventilation flaps (see Figure 2b).

2.2 Default building control

There are two TAC heating circuits in each of the eight building sections (see Figure 1b). These heating circuits are divided by cardinal directions into south/north and south-west/north-west, respectively, resulting in 16 different control loops. By default, all TAC heating circuits are controlled identically. The supply temperature set point follows

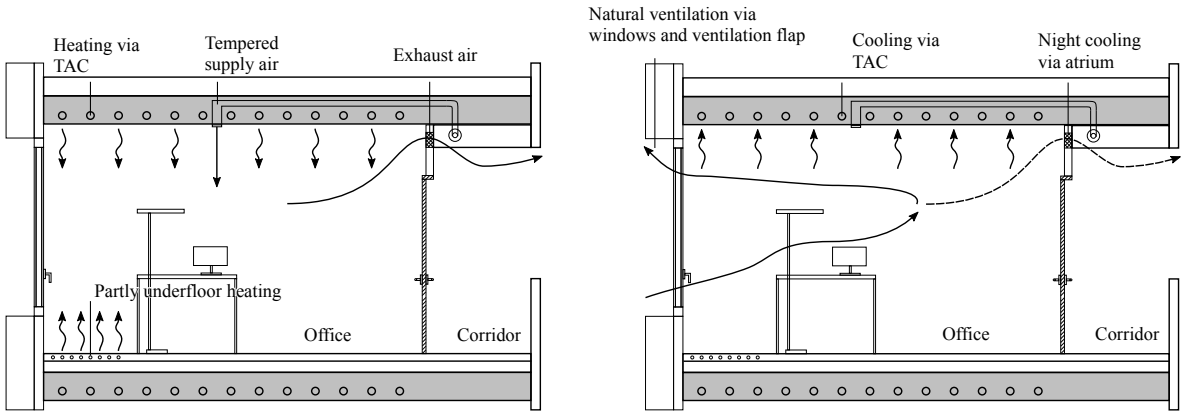

(a) Heating mode **(b)** Cooling mode

Figure 2: Schematic representation of a standard office in heating mode (a) and cooling mode (b)

an outdoor temperature-dependent linear heating or cooling curve. The set point is set by controlling three-way mixing valves with PI controllers in every heating circuit. The circulation pumps of each circuit are activated based on simple time-depend schedules. This type of control is a rule-base control since it follows a simple "IF *event* THAN *action*" principal. Switching from heating to cooling mode operation is done automatically by the building management system based on the averaged outdoor air temperature of the past 36 hours.

2.3 Monitoring system

The building has been continuously investigated as part of a scientific monitoring project since July 2014. The aim of this monitoring was to examine the energy requirement targets and to continuously optimize the building operation with regard to user comfort and operating costs. The results of the monitoring project can be found in (Duus & Schmitz, 2021). The monitoring system comprises an extensive network of more than 1100 sensors, consisting of various energy meters, flow meters and temperature sensors, to measure and record the relevant parameters within the various subsystems at a sampling rate of 1 min. To additionally analyze and evaluate user comfort, 32 *reference office spaces* were equipped with sensors for air temperature, relative humidity, presence and window operation. The collected measurement data from the monitoring system will be used within the framework presented.

3. CONTROLLER BUILDING MODEL

Model Predictive Control (MPC) relies on dynamic models representing the thermal behavior of a building or particular zones within it. The accuracy of these controller models is crucial for the overall performance of the MPC controller (Blum et al., 2019). The simulation time of these models must be reasonably fast, since they are used in an online optimization problem solved almost in real-time.

The development of models that represent the dynamic thermal behavior of buildings and at the same time can be used in real-time control applications is currently still one of the biggest challenge for the implementation of MPC in the building sector (Killian & Kozek, 2016). The classes of building models used here can be characterized as control-oriented models, which were developed specifically for control applications, such as Model Predictive Control (MPC) (Atam & Helsen, 2016).

In this case, the implemented MPC controller uses simplified gray-box models of one or more reference offices as process model for prediction of thermal behavior. This modelling approach is the most widely used method for developing models applied in control applications (Kathirgamanathan et al., 2021). The gray-box-model is shown in Figure 3. It consists of seven resistances and four capacities, known as R7C4 model. The four state variables T_W (exterior wall temperature), T_Z (indoor air temperature or zone temperature), T_{Int} (temperature of internal masses) and T_{TAC} (TAC temperature) correspond to the four capacities C_W, C_{Air}, C_{Int} and C_{TAC}.

For the TAC, a simplified model consisting of two resistances and one capacity based on the EMPA model developed by (Koschenz & Lehman, 2000) is used. For simplification, equal room temperatures below and above the ceiling

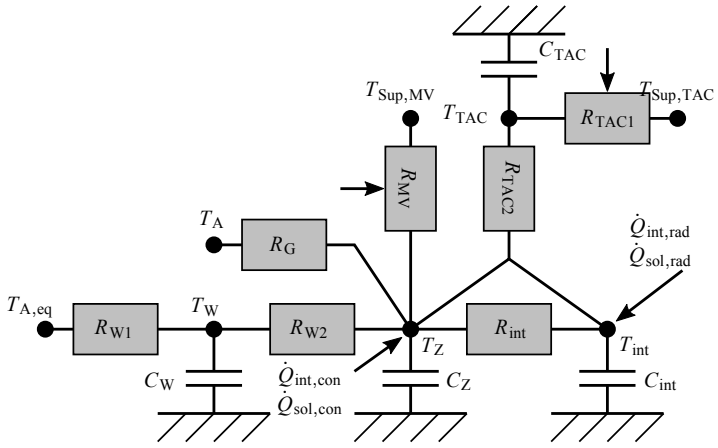

Figure 3: RC-network representation of the used gray-box model.

are assumed so that the two heat flow paths to respectively the room above and below the ceiling can be transformed into a single heat flow path. The external wall is represented by two envelop resistances (R_{W1} and R_{W2}) and one glazing resistance (R_G). Mechanical ventilation is modeled with one resistance R_{MV}. The resistance R_{int} accounts for heat exchange between the air volume and internal masses. Heat exchange between adjacent zones is neglected by assuming similar temperatures in every office.

The model inputs can be divided into (external) disturbances (denoted as **d**) and manipulable control variables (denoted as **u**). The disturbances are the outside air temperature T_A, the global solar radiation on the vertical facade with the corresponding orientation ($\dot{I}_{glo,orient}$) which is split into convective ($\dot{Q}_{sol,con}$) and radiative heat gains ($\dot{Q}_{sol,rad}$), the mechanical ventilation supply temperature ($T_{Sup,MV}$) together with the boolean signal of supply ($z_{Sup,MV}$) and the occupancy signal (*occ*) which acts on the convective ($\dot{Q}_{int,con}$) and radiative ($\dot{Q}_{int,rad}$) internal gains. The control variables used by the MPC controller are the TAC supply temperature ($T_{Sup,TAC}$) and the binary signal (on/off) of the circuit pump ($z_{Sup,TAC}$).

The gray-box zone model shown in Figure 3 is implemented in the equation-based, object-oriented modeling language Modelica (The Modelica Association, 2023). Its system behavior can be represented in the form of an implicit differential-algebraic equation system (DAE)

$$\mathbf{F}\left(\dot{\mathbf{x}}(t), \mathbf{x}(t), \mathbf{y}(t), \mathbf{d}(t), \mathbf{u}(t), \mathbf{\Theta}\right) = 0 \tag{1}$$

where **x** is the state vector, **y** is the output vector defined as the zone temperature T_Z, **d** is the disturbance input vector, **u** is the input vector holding controllable inputs and $\mathbf{\Theta}$ is the (time-independent) parameter vector. A dedicated parameter method is used to identify the values of the model parameters using measured input and output data from previous years of operation. More information about the model and the identification method can be found in (Freund & Schmitz, 2019) and (Freund, 2023).

4. MODEL PREDICTIVE CONTROL FORMULATION

The MPC controller developed is configured as a higher-level controller and takes the role of set point generator for the underlying, unchanged control of the TAC control loops. A TAC control loop consists of a circulation pump, a three-way mixing valve with an associated PI controller, and the distribution system. The MPC controller specifies the set point for the flow temperature $T_{Sup,TAC}$ as well as the on/off signal of the circulation pump $z_{Sup,TAC}$. The measured flow temperature and the measured zone temperatures $T_{Z,i}$ of the reference zones in the respective building section are available to the controller as feedback variables.

The objective of MPC is to minimize the heating energy demand while simultaneously maximizing the thermal comfort. Therefore, the cost function to be minimized consists of three (time-dependent) components: the energy costs J_{ec}, the discomfort costs J_{dc}, and the costs for control input changes $J_{\Delta u}$. The individual components of the cost function can

be weighted using the weighting factors β_{ec}, β_{dc}, and $\beta_{\Delta u}$, thereby determining their importance. Therefore, these weighting factors serve as control parameters, allowing the adjustment of the control behavior. Due to the discrete-time operation of the controller, the system equations of the zone models are discretized in time. The continuous time $t \in [t_0, t_p]$ with t_p as the prediction time is converted into the discrete time $k \in [0, 1, \ldots, N_p - 1]$ at a specified fixed sampling time t_s, whereby $N_p = \frac{t_p}{t_s}$ ts applies to the prediction horizon. All equations are therefore given in discrete-time form. The control horizon N_c is equal to the prediction horizon ($N_c = N_p$). Therefore, the dynamic multi-criteria optimization problem can be generally formulated as follows:

$$\mathbf{u}^*(k) = \arg\min_{\mathbf{u}(k)} \beta_{ec} J_{ec} + \beta_{dc} J_{dc} + \beta_{\Delta u} J_{\Delta u} \tag{2}$$

subject to:

$$F(\dot{\mathbf{x}}_i(k), \mathbf{x}_i(k), \mathbf{y}_i(k), \mathbf{u}(k), \mathbf{d}_i(k), \mathbf{p}_i) = 0 \tag{3}$$

$$\mathbf{u}_{min} \leq \mathbf{u}(k) \leq \mathbf{u}_{max} \tag{4}$$

The dynamic system behavior of the zone models $i = (1, \ldots, n_Z)$ is described by the R7C4 model presented in the previous section, which can be rewritten as an implicit, time-discrete DAE in (3). The inequality constraints (4) for the control input $\mathbf{u}(k)$ are formulated as hard constraints. The lower and upper bounds of the control inputs, $\mathbf{u}_{min}$ and $\mathbf{u}_{max}$, are based on requirements from the considered heating/cooling system. The result of minimizing the cost function is the optimized sequence of the control input $\mathbf{u}^*(k)$ over the prediction horizon N_P.

4.1 Energy cost function

The energy costs consist of the sum of the heating energy used by the TAC for all zone models representing the considered heating circuit, as well as the power consumption of the circulation pump for this circuit. To calculate the total heating energy, the sum of TAC heating output $\dot{Q}_{TAC,i}$ for each zone model $i = (1, \ldots, n_Z)$ is summed over the prediction horizon N_p. For the pump energy, the control variable u_P is summed over the prediction horizon instead of using the pump energy directly. Thereby, only operating times of the pumps are optimized. Both components can be weighted by the factor β_{TAC} and β_P. The energy cost are defined as follows:

$$J_{ec} = \beta_{TAC} \sum_{k=0}^{N_p-1} \sum_{i=1}^{n_Z} \dot{Q}_{TAC,i}(k) + \beta_P \sum_{k=0}^{N_p-1} u_P(k) \tag{5}$$

$$\tag{6}$$

4.2 Discomfort cost function

For the calculation of discomfort costs, soft constraints are used for the control variable zone temperature $T_{Z,i}$. For this purpose, slack variables $\mathbf{s}$ are introduced. These slack variables can also be interpreted as a measure for the violation of a temperature range defined by T_{min} and T_{max}. The slack variables of the considered zones s_i are calculated with the zone weighting factors $\beta_{Z,i}$ to a zone-weighted slack variable $\mathbf{s}_i$. This allows, among other things, to weight the comfort violation of different zones differently and thus to balance uneven zone temperatures between the zones. Furthermore, with the zone weighting factors, it is possible to ignore the comfort violation caused by the short-term temperature drop when opening windows in the discomfort costs, in order to avoid undesired controller behavior. The discomfort costs are therefore defined as:

$$J_{dc} = \sum_{k=0}^{N_p-1} \| s_{zm}(k) \|^2 \tag{7}$$

with

$$s_{zm}(k) = \sum_{i=1}^{n_Z} \beta_{Z,i}(k) \cdot s_i(k) \tag{8}$$

$$T_{min}(k) - s_{i,k} \leq T_{Z,i}(k) \leq T_{max}(k) + s_i(k) \tag{9}$$

$$s_i(k) \geq 0 \tag{10}$$

4.3 Control variable change cost function

The third part of the cost function is the cost of control variable changes. This prevents the optimized control variable from changing excessively fast or frequently. This is especially relevant where the actuator of the real system (in this case, for example, the mixing valve) has a certain dynamic and thus cannot follow sudden changes in the control variable. It can also be used to prevent switching the circulator pumps excessively on and off. The cost of a control variable change is defined as:

$$J_{\Delta u} = \sum_{k=0}^{N_\mathrm{p}-1} \|\Delta u(k)\|^2 \tag{11}$$

with

$$\Delta u(k) = u(k) - u(k-1) \tag{12}$$

5. RESULTS AND DISCUSSION

The proposed MPC controller was implemented in the low-rise buildings sections A, C and G (see Figure 1b) and therefore substituted the RBC of the two existing TAC heating circuits in this building sections. The experiment was conducted from November 2020 to April 2021. The MPC controller was used in section G throughout the entire duration, whereas the controllers in section A and section C were implemented in December and January, respectively. The other building sections remained in RBC operation. This configuration allows a direct and detailed comparison of MPC and RBC controller performance in similar building sections and under identical operating conditions.

Table 1 provides an overview of the floor areas, the number of offices, and the number of existing reference zones in the examined buildings A, C, and G. In each building, two TAC heating circuits exist which are independently controlled. The evaluation of heating energy demand and thermal comfort is carried out for the entire building section, as only one heat meter is available per building. The measurement uncertainty of the heat meters is ±6 % of reading.

Table 1: Overview of the heated area, number of offices and reference zones in the buildings A, C and G.

Building	Heating circuit	Heated area	Number of offices	Number of reference zones
A	North-East	681 m^2	39	2
	South-West	1339 m^2	62	3
C	North-East	692 m^2	41	2
	South-West	1001 m^2	55	3
G	East	890 m^2	67	2
	West	1380 m^2	107	5

5.1 Heating energy

To determine the influence of the MPC control on the heating energy demand compared to the default RBC control, a two-step correction of the heating energy step achieved is done. First, all heating energy demands are outdoor-temperature corrected according to (VDI 3807, 2013) using heating degree days and related to the heated floor area. In a second step, the measured heating energy demand is related to an “expected” heating energy demand for the evaluation period. This expected heating energy demand is determined based on the average value for the past six years of operation (2015 to 2020) and corrected by the ratio of the heating energy demand for the evaluation period to the six-year average of the RBC controlled building sections. Thus, this expected heating energy demand represents the demand for an MPC controlled building section that is expected with RBC control. The approach takes into account that, besides the outside temperature, there are other influencing factors that can affect the heating energy demand of the building. Examples of these are changes in building operation or changes in usage behavior and internal heat gains.

Figure 4 shows the expected and measured monthly area-specific heating energy demand q_H of the three MPC controlled building sections A, C, and G. As described earlier, MPC control was activated in House A in December and

in House C in January. As expected, the heating energy demand is highest in January and lowest in April. Except for November in Building G, the measured heating energy demand during the MPC controlled heating season consistently remained lower than the expected heating energy demand. The resulting relative and absolute savings in heating energy are presented in Table 2.

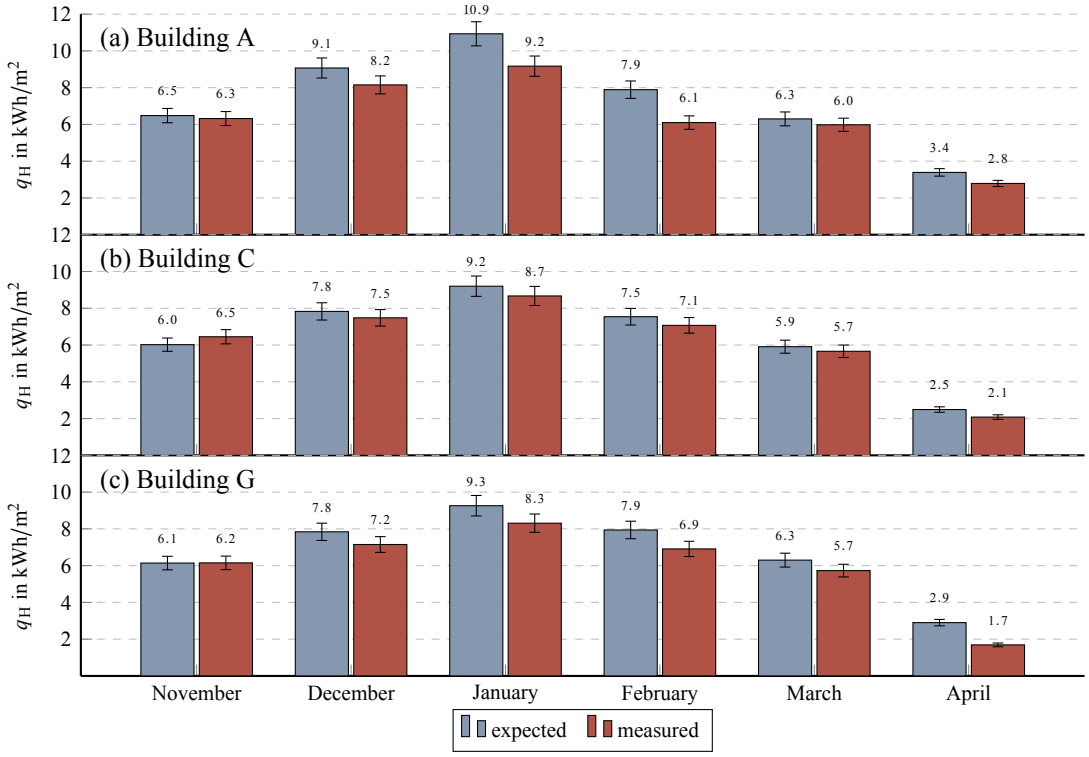

Figure 4: Expected and measured TAC heating energy demand of the MPC-controlled sections.

For Building A, savings ranging from 5 % in March to 22 % in February are achieved. In comparison, the lowest savings of 4 % to 16 % are achieved for Building C. In November, a very slight increase in heating energy demand of 0.1 percent is observed for Building G. In April, the highest savings of 41 % are achieved for Building G. The overall heating energy savings over the entire six months period amount to 11.2 % relative and 26 134 kWh absolute.

Table 2: Absolute and relative savings in heating energy for sections A, C and G. In section A, the MPC control was activated in December, in house C in January (fields in gray show the months with RBC control).

Month	Build. A		Build. C		Build. G	
	abs. (kWh)	rel. (%)	abs. (kWh)	rel. (%)	abs. (kWh)	rel. (%)
November	340	2.59	−580	−5.1	−15	−0.1
December	1864	10.2	−336	−2.15	1844	8.8
January	3561	16.1	1060	5.8	2546	10.3
February	3611	22.7	827	6.2	2443	12.9
March	654	5.1	459	4.3	1412	9.1
April	1215	17.8	936	16.5	3717	41.7
Total	10 906	14.4	3282	6.8	11 946	11.4

The benefits and performance of an MPC controller are particularly pronounced in highly variable weather conditions,

i. e. high day/night differences in outdoor temperature, high solar irradiation or generally changing weather conditions. The reason for this is that the default RBC determines the supply temperature set point based on relatively cold outside air temperature during nighttime, resulting in high set point values and high heating power. In contrast, the MPC controller "knows" about the high daytime air temperature and the high solar irradiation of the following day, which leads to anticipatory behavior with low set point values and heating activity respectively. These fluctuating weather conditions occur typically in transitional months such as April. February was also characterized by an alternation of very cold and exceptionally warm periods, with a wide temperature range from -10 °C to 20 °C within a week. Consequently, the highest energy savings were achieved in these two months.

Both between the individual buildings and between the individual months, a significant difference can be seen in terms of controller performance. The potential for heating energy savings is greatest in Building A with 14.4 % and lowest in Building C with 6.8 %. A possible reason for this can be found in the heterogeneous distribution of room temperatures within the reference zones of House C, see Figure 5. The range of prevailing room temperatures in Building C is considerably wider in comparison to the other buildings. As the controller aims to regulate room temperatures in all reference zones above the lower temperature limit (gray lines), a wide, heterogeneous room temperature distribution results in a lower optimization potential for heating energy savings.

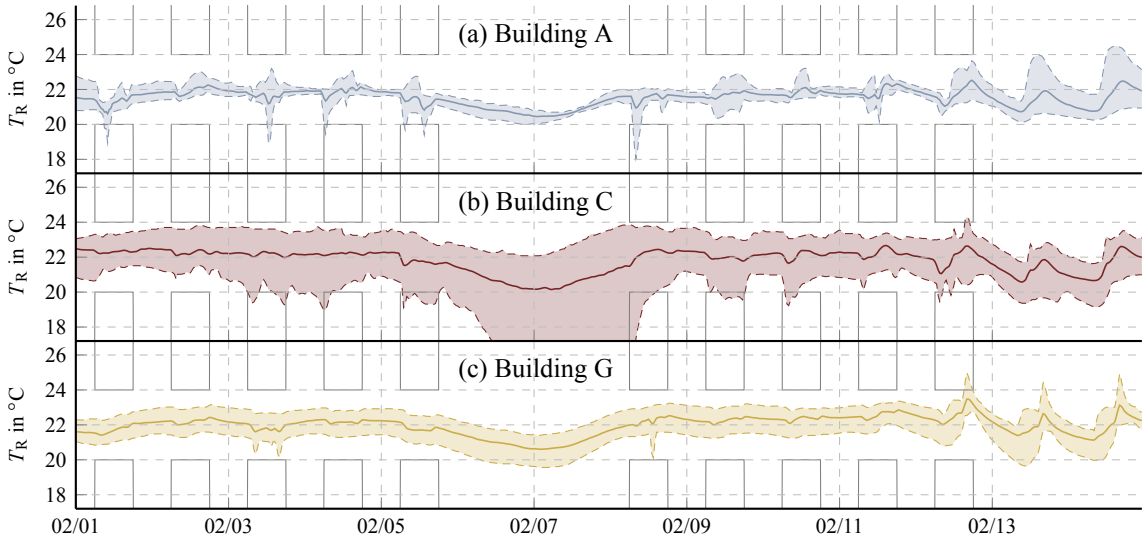

Figure 5: Measured temperature range in reference zones of building sections A, C and G in February. Solid lines are mean values, dashed lines represent minimum and maximum values.

Another cause, which can be seen in Figure 5 is the influence of user behavior. A pronounced temperature drop over the weekend, caused by prolonged opening of windows for several days, can be identified. This user behavior is beyond the normally expected behavior and has a negative impact on the controller performance, both in terms of heating energy savings and thermal comfort, as described in the next section.

5.2 Thermal comfort

For the evaluation of thermal comfort, the measurement data for room temperatures in the reference zones on the third floor of Houses A, C, and G are considered. For the evaluation, the percentages of the room air conditions are evaluated here based on the comfort room temperature defined in accordance with (DIN EN 16798, 2022). The comfort room temperature is set to 22 °C, the allowed deviations are defined as ±1 K, ±2 K and ±3 K for categories I, II and III respectively. Room air conditions with a larger deviation as 22 °C ± 3 °C are denoted as category IV. Violation of these comfort bounds is only counted during working hours (Monday to Friday from 6am to 6pm). Figure 6 shows the shares of the comfort categories according to DIN EN 16798 in the seven years of building operation from 2015 to 2021. The evaluation period corresponds to the period of active MPC control in the years 2020 to 2021 (see Table 2). This allows the thermal comfort achieved with MPC and RBC control to be compared directly.

In buildings A and G, the highest percentage of category I (i. e. 22 °C ± 1 °C) compared to all operating years is achieved

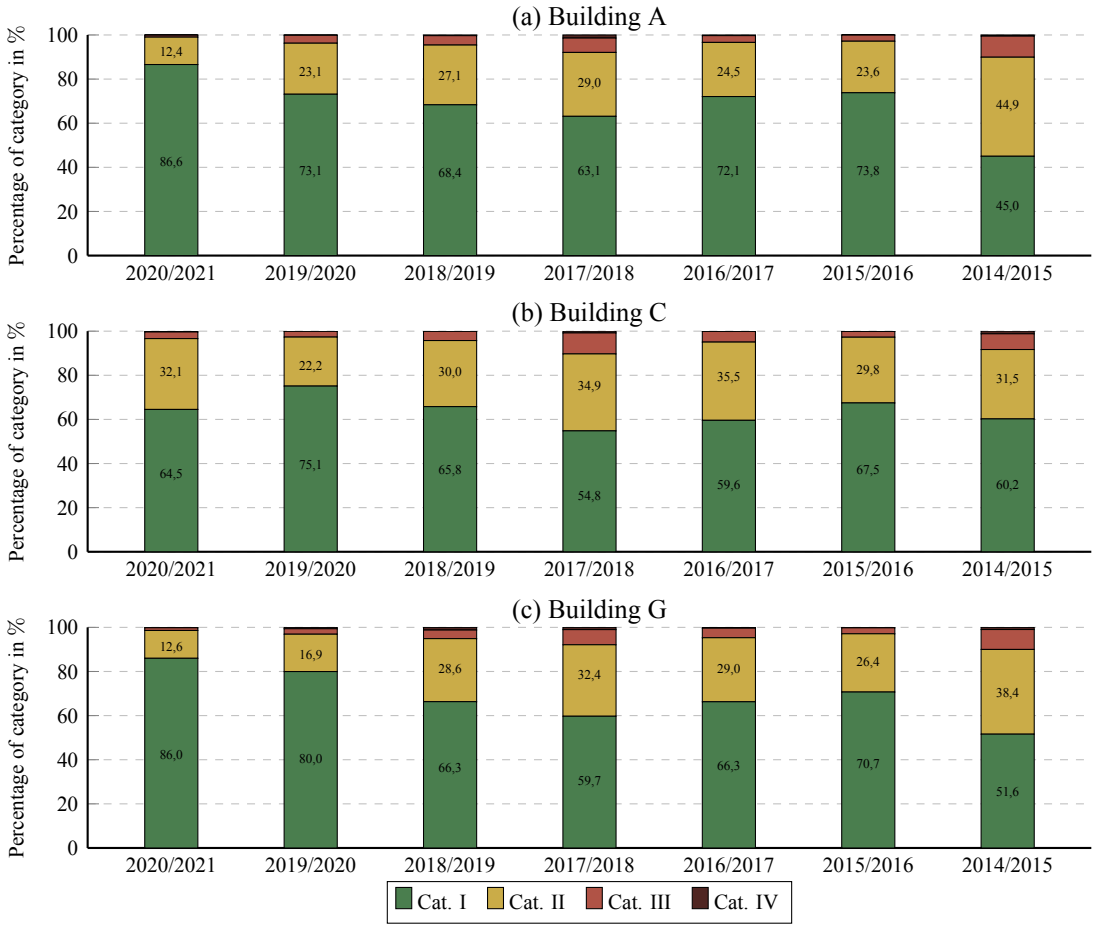

Figure 6: Share of indoor air conditions in the comfort categories in the operating years 2014 to 2021 based on the measured room temperatures in the reference zones.

in the 2020/2021 heating period with 86 %. Moreover, the category II, which is applicable to the building, is met here in 99 % of operational time. Therefore, a clear improvement in thermal comfort can be demonstrated for buildings A and G with regard to a higher share of category I room air conditions with the use of the MPC control strategy.

In contrast, the results are different in Building C. At 64 %, there is no clear increase in the proportion of category I compared to previous years. However, category II is achieved in around 97 % of the usage time, which is comparable to the previous operating years. As already explained before, this results from the inhomogeneous temperature distribution in the reference zones of Building C and possibly a poorer prediction accuracy of the reference zone models due to the influence of occupants. Besides resulting in lower heating energy savings, this also leads to limitations in meeting comfort bounds. Nevertheless, the thermal comfort in Building C during the heating season 2020/2021 is not noticeably worse than in previous years.

6. CONCLUSIONS

This paper describes the real-world implementation of model predictive control in a large-sized office building, controlling the supply temperature and circulation pump of heating circuits for thermoactive ceilings. The core of this MPC strategy consists of gray-box models that describe the dynamic thermal behavior of several reference zones. The cost function of the controller is the weighted sum of the heating energy demand and the thermal discomfort, resulting in a constrained non-linear optimization problem.

In comparison to the conventional, heating-curve-based control strategy, monthly average savings in heating energy

ranging from 5 % 42 % can be measured during the six-month period under investigation. However, the potential for savings is dependent on the prevailing weather conditions. The highest savings can be achieved in transitional months like April, when there are large amplitudes in outside temperature and high solar irradiation. In terms of thermal comfort, a significant improvement in building sections A and G compared to the previous six years of operation can be identified. A significantly higher proportion of indoor air conditions within comfort category I according to DIN EN 16798 is achieved. In contrast, building section C does not show a significant improvement in comfort, which can be attributed to an inhomogeneous distribution of room temperatures within the reference zones and occupant behavior.

REFERENCES

Atam, E., & Helsen, L. (2016). Control-oriented thermal modeling of multizone buildings: Methods and issues: Intelligent control of a building system. *IEEE Control systems magazine*, *36*(3), 86–111.

Blum, D., Arendt, K., Rivalin, L., Piette, M., Wetter, M., & Veje, C. (2019). Practical factors of envelope model setup and their effects on the performance of model predictive control for building heating, ventilating, and air conditioning systems. *Applied Energy*, *236*, 410–425.

Deutsches Institut für Normung. (2022). *Energy performance of buildings - ventilation for buildings - part 1: Indoor environmental input parameters for design and assessment of energy performance of buildings addressing indoor air quality, thermal environment, lighting and acoustics* (No. 6007). Berlin: Beuth Verlag.

Drgoňa, J., Arroyo, J., Figueroa, I. C., Blum, D., Arendt, K., Kim, D., … others (2020). All you need to know about model predictive control for buildings. *Annual Reviews in Control*, *50*, 190–232.

Duus, K., & Schmitz, G. (2021). Experimental investigation of sustainable and energy efficient management of a geothermal field as a heat source and heat sink for a large office building. *Energy and Buildings*, *235*, 110726.

Freund, S. (2023). *Modellbasierte prädiktive regelung komplexer gebäudetechnischer anlagen zur optimierung der energieeffizienz und des komforts* (Unpublished doctoral dissertation). Technische Universität Hamburg.

Freund, S., & Schmitz, G. (2019). Development of a framework for model predictive control (mpc) in a large-sized low-energy office building using modelica grey-box models. In *Building simulation 2019: 16th conference of ibpsa, rome, italy* (pp. 2864–2871).

Freund, S., & Schmitz, G. (2021). Implementation of model predictive control in a large-sized, low-energy office building. *Building and environment*, *197*, 107830.

Gyalistras, D., Gwerder, M., Oldewurtle, F., Jones, C., & Morari, M. (2010). Analysis of energy savings potentials for integrated room automation. In *Clima-rheva world congress.*

IEA. (2023). *Tracking clean energy progress 2023.* IEA Paris. Retrieved from `https://www.iea.org/reports/tracking-clean-energy-progress-2023`

Kathirgamanathan, A., De Rosa, M., Mangina, E., & Finn, D. P. (2021). Data-driven predictive control for unlocking building energy flexibility: A review. *Renewable and Sustainable Energy Reviews*, *135*, 110120.

Killian, M., & Kozek, M. (2016). Ten questions concerning model predictive control for energy efficient buildings. *Building and Environment*, *105*, 403–412.

Koschenz, M., & Lehman, B. (2000). *Thermoaktive bauteilsysteme tabs* (1. Aufl. ed.). Dübendorf: EMPA Energiesysteme/Haustechnik.

Serale, G., Fiorentini, M., Capozzoli, A., Bernardini, D., & Bemporad, A. (2018). Model predictive control (mpc) for enhancing building and hvac system energy efficiency: Problem formulation, applications and opportunities. *Energies*, *11*(3), 631.

Sofos, M., Langevin, J., Deru, M., Gupta, E., Benne, K. S., Blum, D., … Widergren, S. (2020). *Innovations in sensors and controls for building energy management: Research and development opportunities report for emerging technologies.* doi: 10.2172/1601591

The Modelica Association. (2023). *Modelica.* Modelica Association. Retrieved from `https://www.modelica.org/`

Thieblemont, H., Haghighat, F., Ooka, R., & Moreau, A. (2017). Predictive control strategies based on weather forecast in buildings with energy storage system: A review of the state-of-the art. *Energy and Buildings*, *153*, 485–500.

Treado, S., & Chen, Y. (2013). Saving building energy through advanced control strategies. *Energies*, *6*(9), 4769–4785.

Verein Deutscher Ingenieure. (2013). *Characteristic consumption values for buildings - fundamentals* (No. 3807). Berlin: Beuth Verlag.